Computer Communications 193 (2022) 176–188

Contents lists available at ScienceDirect

Computer Communications

journal homepage: www.elsevier.com/locate/comcom

Using self-deferral to achieve fairness between Wi-Fi and NR-U in downlink and uplink scenarios

Szymon Szott [a,*], Katarzyna Kosek-Szott [a], Alice Lo Valvo [b], Ilenia Tinnirello [c,d]

[a] AGH University of Science and Technology, Krakow, Poland
[b] Prysmian Electronics S.r.l., Prysmian Group S.p.A., Palermo, Italy
[c] University of Palermo, Palermo, Italy
[d] Consorzio Nazionale Interuniversitario per le Telecomunicazioni (CNIT), Italy

ARTICLE INFO

Keywords:
Wi-Fi
LAA
NR-U
Coexistence
Machine learning

ABSTRACT

Wireless networks operating in unlicensed bands generally use one of two channel access paradigms: random access (e.g., Wi-Fi) or scheduled access (e.g., LTE License Assisted Access, LTE LAA and New Radio-Unlicensed, NR-U). The coexistence between these two paradigms is based on listen before talk (LBT), which was, however, designed for random access. Meanwhile, scheduled systems require that their transmissions start at the beginning of a slot boundary. Synchronizing this boundary to the end of LBT usually requires transmitting a reservation signal (RS) to block the channel. Since the RS is a waste of channel resources, we investigate an alternative self-deferral approach (gap-based access) using analytical and simulation models. We put forth a proposal to employ only self-deferral, treat the gap mechanism as a partial backoff, and adjust the contention window (CW) settings to the number of coexisting nodes. We demonstrate that this approach not only ensures fairness in Wi-Fi/NR-U coexistence but also avoids wasting radio channel resources and improves aggregate network throughput. Furthermore, we show that the proposed approach outperforms RS-based access and provides significant throughput and fairness gains. Finally, we implement a long short-term memory-based (LSTM) regression model to predict those Wi-Fi/NR-U CW settings which lead to coexistence fairness.

1. Introduction

Wireless networks operating in unlicensed bands generally use one of two basic paradigms: random access (e.g., Wi-Fi) and scheduled access (e.g., LTE License Assisted Access, LTE LAA and New Radio-Unlicensed, NR-U). The coexistence between these two paradigms has gained much attention from the academic community in recent years (cf. Section 2). Despite research efforts, however, the problem remains an important challenge, as confirmed by recent measurement-based studies [1,2].

Coexistence between Wi-Fi and NR-U is based on having both technologies perform a listen before talk (LBT) procedure before accessing the channel [3]. LBT is considered fairer in comparison to duty cycling used by LTE-U [4] but it was designed for random channel access whereas scheduled systems require that their transmissions start at the beginning of a slot boundary [5]. Synchronizing this boundary with the end of LBT requires that either (a) channel access is initialized after a self-deferral (i.e., *gap period*) which is not interrupted by some other transmission or (b) the NR-U node transmits a *reservation signal* (RS) which blocks the channel until the start of the slot boundary (Fig. 1). The RS-based approach is often used in coexistence analyses, but it is not explicitly mentioned in 3GPP specifications [6]. Additionally, it has been criticized not only by IEEE [7] but also by researchers [5,8,9] as a potential source of bandwidth inefficiency. The gap mechanism, however, does not always preserve fairness in coexistence between scheduled and random-access systems [10].

To study this problem, we first develop analytical and simulation models (Section 4). Then, we put forth a proposal to employ only self-deferral (for NR-U), treat the gap mechanism as a partial backoff (during LBT), and use contention window (CW) settings adjusted to the number of coexisting nodes (Section 5). We demonstrate that this approach not only ensures fairness in Wi-Fi/NR-U coexistence but also avoids wasting radio channel resources and improves aggregate network throughput. Furthermore, we show that the proposed approach outperforms RS-based access and provides significant throughput and fairness gains. Finally, we implement a long short-term memory-based (LSTM) regression model to predict those Wi-Fi/NR-U CW settings which lead to coexistence fairness (Section 6).

* Correspondence to: AGH University of Science and Technology, Faculty of Computer Science, Electronics and Telecommunications, al. A. Mickiewicza 30, 30-059 Krakow, Poland.
E-mail addresses: szott@agh.edu.pl (S. Szott), kks@agh.edu.pl (K. Kosek-Szott), alice.lovalvo@prysmiangroup.com (A. Lo Valvo), ilenia.tinnirello@unipa.it (I. Tinnirello).

https://doi.org/10.1016/j.comcom.2022.06.040
Received 11 March 2022; Received in revised form 25 May 2022; Accepted 26 June 2022
Available online 4 July 2022
0140-3664/© 2022 The Author(s). Published by Elsevier B.V. This is an open access article under the CC BY license (http://creativecommons.org/licenses/by/4.0/).

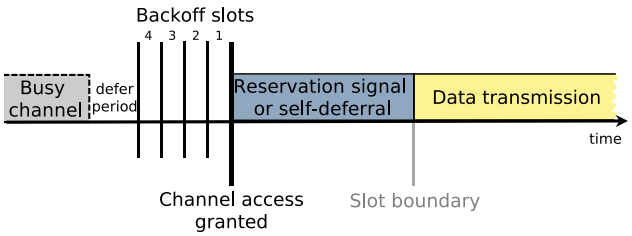

Fig. 1. Two approaches to aligning an LBT procedure with the slot boundary of a scheduled access network such as NR-U: reservation signal or self-deferral (gap).

This article extends our previous results presented in [11]. Here, we generalize the contributions done by the following:

- We show that no static CW settings satisfying the requirement of high channel utilization and fairness can be considered universally applicable (Section 5.5).
- We extend our previous analytical and simulation models of downlink transmissions with uplink transmissions (Section 7).
- We show through simulations that the proposed approach has certain limitations when ensuring fairness in uplink scenarios (Section 7.1) and we suggest a viable solution (Section 7.2).
- We show in Section 6 that the regression model can be trained not only with data from the simulation model but also with data from the analytical model to predict Wi-Fi/NR-U CW settings resulting in coexistence fairness.

We conclude with a summary of the findings and outline future work in Section 8.

2. State of the art

The coexistence between random (Wi-Fi) and scheduled-based (LAA, NR-U) access in shared channels has been intensely studied in recent years [12]. So far, most works have focused on Wi-Fi/LAA coexistence and assumed that LAA uses RSs, e.g., [13–19]. Meanwhile, research shows that LAA performance is strikingly different under self-deferral [10,20,21].

In a recent trend, researchers have started to propose augmenting cellular networks with machine learning (ML) techniques to improve channel allocation, transmission scheduling, and coexistence fairness. Typically, they propose changes to the standard LTE-U/LTE-LAA operation or provide new ways of monitoring Wi-Fi conditions and traffic demands [22–29]. An overview of applying ML-based solutions for Wi-Fi and cellular coexistence can be found in [30].

An alternative approach is to modify the standard LBT scheme. Saadat et al. suggest tuning the CW and TXOP parameters based on the observed network load to improve the overall performance [31]. In terms of maintaining coexistence, instead of using an RS, they have LAA eNBs send a CTS-to-self frame to inform Wi-Fi nodes of their impending transmissions. The CTS-to-self mechanism is also considered by Candal-Ventureira as an exemplary method of achieving time multiplexing between Wi-Fi and LAA [32]. In contrast to the previous proposal, however, they have the Wi-Fi AP send the frame to reserve the channel for LAA. Meanwhile, Han et al. [33] propose to intelligently tune CWs for both LAA and Wi-Fi nodes using reinforcement learning. However, they assume that LAA nodes start transmitting immediately after LBT. Ali et al. also tune CW parameters but using neural networks [22]. They assume RS-based channel access but also consider issues related to collisions and updating the CW, including the impact of delayed CW update due to LTE's HARQ.

Adaptive contention window tuning with a selection of the maximum transmission duration is also proposed in [34]. The authors focus on maximizing the total network throughput. However, such an approach is based on a constant synchronization delay for LAA and promotes nonstandard behavior.

Huang et al. [35] address the impact of hidden and exposed nodes on Wi-Fi/LAA coexistence. They propose a receiver-initiated transmission mode for LAA (based on a design for mmWave networks [36]), which can reduce the collision rate and improve the throughput. However, following [36], they do not consider the necessity of LAA transmissions to be synchronized to slot boundaries. For mmWave bands, this requirement can be lifted, especially if the slot length is short. However, this is not the case for the 5 GHz band. Lee and Yang also address the impact of hidden nodes by applying transmit precoding and power control on the LAA side [37] but without mentioning the need for synchronization to slot boundaries.

Saleem et al. [38] suggest completely avoiding inter-network collisions by having Wi-Fi and LAA transmit in duty cycles. The authors define the optimization problem and solve it analytically. Again, the synchronization slot boundaries are not considered. Furthermore, Loginov et al. suggest an alternative LBT implementation, which does use RSs, but in a new way, in the form of short busy tones [39,40]. This provides collision detection and resolution which leads to increased network performance, at the cost of changes in LAA/NR-U channel access behavior. Another way to improve the coexistence between Wi-Fi and LAA is by controlling the transmit power. Kushwaha et al. provide a method that considers multi-channel operation, but their analysis does not examine the impact of slot boundaries [41].

Furthermore, in the topic of coexistence between NR-U and Wi-Fi, Naik et al. [42] discuss issues in the 6 GHz band, while the authors of [43–46] provide coexistence studies for the mmWave (60 GHz) band. In particular, [42] is a tutorial paper, in which challenges and opportunities for the next generation Wi-Fi and 5G NR-U in the 6 GHz bands are described. Additionally, [43] presents a simulation model developed for ns-3, which takes into account both LBT and duty cycle (LTE-U-like) channel access modes for NR-U. Such a duty cycle duration can be optimized with reinforcement learning [47] or with mixed-integer quadratic programming [48] to improve coexistence. Furthermore, [44] finds stochastic models for SINR and data rate under the assumption of downlink transmissions. Finally, the authors of [46] perform joint frequency and spatial resource allocation to minimize cross-technology interference.

In summary, most of the literature either does not consider slot boundaries or assumes the use of RS-based channel access. Our goal is to find a solution that would take into consideration the characteristics of NR-U transmissions but without resorting to reservation signals.

3. Channel access rules

Channel access for both Wi-Fi and NR-U follow the LBT procedure defined in ETSI specification EN 301 893 [49]. Before transmitting, nodes are required to perform LBT by observing the channel to be idle for 16 μs, referred to as the short inter-frame space (SIFS) in Wi-Fi. Afterwards, contention is resolved by having nodes wait for a fixed and random amount of 9 μs backoff slots. By default (i.e., for best-effort traffic), there are three fixed slots (referred to as the arbitration inter-frame space number, AIFSN in Wi-Fi) and a random number of backoff slots chosen between zero and the current CW value, which is set to CWmin after each successful transmission and doubled (up to CWmax) before each retransmission.

The IEEE 802.11-2016 [50] (Wi-Fi) channel access rules closely follow these LBT specifications. Furthermore, since Wi-Fi requires in-band signaling to confirm unicast transmissions, each successful transmission is followed by an immediate acknowledgment (ACK) frame transmission.

3GPP Rel-16 [6] (NR-U) also follows the LBT rules, where the above-mentioned exponential backoff mechanism is used for data (Cat

−4) transmissions. However, NR-U differs from Wi-Fi in two important aspects. First, acknowledgments are sent over the licensed band.[1] Second, NR-U uses slot-based scheduling: transmissions are organized into radio frames, each composed of 10 sub-frames (slots) and NR-U transmissions can start only at slot boundaries. This requires alignment between the LBT procedure and slot boundary, which can be resolved using a gap period or a reservation signal (RS) transmission (Fig. 1). The primary focus of this study is improving fairness when NR-U uses gap-based channel access, which allows avoiding unnecessary channel occupation by the RSs. The gap can be placed before or after the backoff countdown [10]. We assume the former approach as in [51]. This assumption should not impact the results, as one study observed: "gap placement (either before or after the backoff period) does not play a critical role" [52].

While NR-U slots are by default 1 ms long, NR-U allows for flexible slot length by increasing the subcarrier spacing. For the 5 GHz bands, the slot length can be configured to 250 μs or 500 μs. In addition to this slot-based scheduling, NR-U introduces the concept of mini-slots for non-slot-based scheduling [10], but we do not consider these aspects in this paper.

3.1. Transmission directions

Wi-Fi and NR-U nodes are allowed to perform downlink (DL) and uplink (UL) transmissions in the shared channel. In the case of DL transmissions, APs and gNBs access the channel using LBT. In the case of UL transmissions, the operation can be as follows:

- NR-U gNBs trigger all uplink transmissions and, therefore, only gNBs contend for channel access using LBT.
- Under legacy 802.11 operation, each Wi-Fi station uses LBT to access the channel before a UL transmission.
- Under 802.11ax operation, the AP may use triggered uplink access (TUA) by transmitting trigger frames (TFs) to initiate UL transmissions. Therefore, in TUA only APs contend for the channel. For more details on TUA, we refer readers to [53].

An additional minor difference between DL and UL channel access is the contention parameter values. In particular, the maximum allowed CW value for the best effort traffic is larger for UL (CWmax = 1023) than for DL (CWmax = 63). For more information on the details of channel access parameters, we refer readers to [10].

4. Modeling downlink operation

In this section, we develop analytical and simulation models of Wi-Fi/NR-U coexistence under DL transmissions. In Section 7, we will discuss the changes required to support UL transmissions.

4.1. Analytical model

The main assumptions of our model are the following. First, all devices are within hearability range (i.e., there are no hidden nodes). This means that the end of a data transmission resets the channel state for all nodes (i.e., they all simultaneously begin to count the AIFS time, etc.). Second, the network operates under saturation conditions (i.e., a full-buffer traffic model in all nodes), which means that transmissions occur consecutively on the channel. Third, there are only downlink transmissions, i.e., initiated by Wi-Fi access points (APs) or NR-U base stations (next generation NodeBs, gNBs). Under these assumptions, the channel activity can be described in consecutive contention rounds, including an *idle time* required for solving the contention, as well as a *transmission time*, in which the winner node holds the channel (as shown in Fig. 2).

We propose to model the behavior of each contending node k by deriving the steady-state distribution $B_k(.)$ of the random process $b_k(.)$ which describes the evolution of the backoff counter value at the end of each transmission/collision event delimiting the contention round. Each discrete time $n = 1, 2, \ldots$ identifies the start of the nth contention round, in which the node with the shortest backoff expiration time gains the right to perform a transmission attempt. Such a backoff expiration time depends simply on the backoff counter for Wi-Fi nodes, while for NR-U nodes it also depends on the additional gap interval. Based on previous studies [10], the gap interval can be considered as a random variable, uniformly distributed between 0 and the maximum synchronization slot Δ (in μs). In the model, we measure this value in backoff slots: $\Delta_s = \Delta/9$ μs. For simplicity, we assume that all nodes use a constant (but adjustable) CW, to better clarify the impact of the random gap interval on the contention process. Generalizations to exponential backoff mechanisms are straightforward. To some extent, the contention process between Wi-Fi and NR-U nodes is similar to the contention process between two access categories (ACs) of the enhanced distributed channel access (EDCA) defined in the IEEE 802.11 standard, in which the arbitration inter-frame space (AIFS)[2] value used by one service class (corresponding to NR-U nodes) is a random variable (equivalent to gap interval+$AIFS_{\mathrm{BE}}$ interval for the best effort (BE) traffic) rather than a fixed interval.

To model Wi-Fi/NR-U coexistence, we use an approach similar to the one proposed in [54]. Let N be the total number of contending nodes, with N_W Wi-Fi nodes (APs) and $N_N = N - N_W$ NR-U nodes (gNBs). Let β_k be the additional gap interval (measured in backoff slots) required by each kth contenting node for starting a transmission attempt on the channel. Such a value is equal to zero for Wi-Fi nodes, which can start transmitting immediately after the expiration of the backoff counter. Conversely, for NR-U nodes we assume it is a random variable, uniformly distributed between 0 and Δ_s, which represents the difference between the starting time of the next available synchronization slot and the backoff expiration time.

The idle time required for starting a new transmission on the channel in the current contention, expressed in the number of backoff slots, is equal to:

$$\delta(n) = \min_{j=1,2,\ldots N} [b_j(n) + \beta_j(n)]. \tag{1}$$

Note that channel access times for NR-U nodes are not in general synchronized with channel access times for Wi-Fi nodes, because the gap interval is not necessarily an integer number of backoff slots. Let CS be the carrier sensing time (which we assume equal to one half backoff slots) and ξ be the nodes whose backoff expiration time is in the interval $\delta(n) + CS$, i.e., the nodes starting a new transmission attempt in the current contention. The backoff evolution law can be defined as:

$$b_k(n+1) = \begin{cases} b_k(n) - \lceil \delta(n) \rceil, k \notin \xi \\ \quad \text{for Wi-Fi,} \\ b_k(n) - \max\{\lceil \delta(n) - \beta_k(n) \rceil, 0\}, k \notin \xi \\ \quad \text{for NR-U,} \\ rand(CW_k), k \in \xi, \end{cases} \tag{2}$$

where $rand(CW_k)$ is an integer extracted randomly in the range $[0, CW_k]$, where CW_k is the CW used by node k.

Fig. 2 shows an example of the backoff evolution process of one Wi-Fi and one NR-U node in three consecutive contention rounds. In the first round, the Wi-Fi node expires first its backoff counter equal to 3 slots, while the NR-U node keeps its backoff counter frozen (where the gap is longer than the backoff expiration time). A new random backoff counter equal to 7 is extracted for the next round. In the second round, the NR-U node has a smaller access time and wins the

[1] NR-U, like LAA, is based on carrier aggregation with devices having a connection in both licensed and unlicensed bands [3].

[2] For each AC, $AIFS_{\mathrm{AC}}$ is calculated as: $AIFSN_{\mathrm{AC}}$ times the backoff slot length plus SIFS.

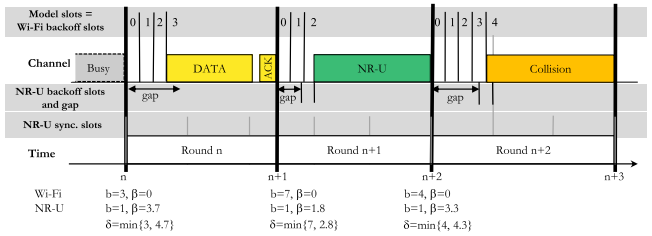

Fig. 2. An example of the backoff evolution process in a coexistence scenario with one Wi-Fi and one NR-U node. The channel is divided into contention rounds, which in turn include an idle contention time, indexed in consecutive backoff slots b, and a final channel holding time (i.e., the time required to transmit a Wi-Fi DATA and ACK frame or a series of NR-U subframes). Note that the model slots are enumerated in ascending order, whereas the Wi-Fi backoff slots are usually numbered in descending order.

contention, thanks to a new gap value equal to 1.8 backoff slots. Since the NR-U transmission is performed after two idle slots from the last transmission, the Wi-Fi backoff counter is decremented by three units. Finally, in the last contention round, the two nodes collide, although their access times do not coincide exactly. This is due to the required channel sensing time CS.

4.1.1. Per-node backoff process

Consider now the evolution of the backoff process of a tagged Wi-Fi node w at the end of a contention. We sequentially index the idle backoff slots that follow our model time as slot 0, 1, …, M, as well as the channel holding time concluding each contention, as shown in Fig. 2. The number of backoff idle slots in each contention is bounded by the minimum value among the maximum contention time of each node, i.e., $M = \min\{CW_w, CW_n + \lceil \Delta_s \rceil - 1\}$. Assume that we know the probability $T_w(i)$ that any other node starts its first transmission attempt in the ith slot. We remark that each transmission attempt is not in general synchronized to the start of a new backoff slot, because of the gap interval employed by NR-U nodes. For example, in the last contention round illustrated in Fig. 2, the NR-U node starts its transmission after 4.3 idle slots from the end of the previous channel holding time (i.e., within the slot numbered as 4, but not exactly at the start of such a slot).

For Wi-Fi nodes, we can characterize the steady-state backoff probability $B_w(j)$ to have a backoff counter equal to j as follows:

$$B_w(j) = \sum_{r=1}^{CW_w - j} B_w(j+r) \cdot T_w(r-1) + \\ + \frac{1}{CW_w} \cdot \sum_{r=0}^{CW_w} B_w(r) \cdot \left[1 - \sum_{l=0}^{r-1} T_w(l) \right]. \tag{3}$$

Note that if 0 is the randomly chosen backoff ($r = 0$), then the last summation of $T_w(l)$ in (3) is evaluated as 0.

At the end of a new contention round, the backoff counter of the tagged node w may be equal to j for two different reasons:

- it has been decremented to j starting from a greater value $j + r$ (with $r \in \{1, 2, \ldots, CW_w - j\}$), because a transmission attempt has been performed by other nodes in the $r - 1$ slot;
- it has been randomly set to a new value equal to j right after a transmission attempt performed by the tagged node.

Note that the expiration of a generic backoff counter equal to r occurs when no other node transmits in the consecutive slots numbered from 0 to $r - 1$. This happens with probability $1 - \sum_{l=0}^{r-1} T_w(l)$.

For NR-U nodes, at each contention round, the backoff process is resumed only after the expiration of the gap interval. Therefore, assuming we know the $T_n(i)$ probability that a tagged NR-U node n sees a transmission performed by other nodes within the ith slot, the backoff counter is updated only when i is greater than β_n. Let $G(i)$ be the probability that the random gap is in the interval between i and $i + 1$ backoff slots, with $i \in \{0, 1, \ldots, \lceil \Delta_s \rceil - 1\}$. In other words, we approximate such a probability with a uniform discrete distribution, whose generic value $G(i)$ is equal to $1/\lceil \Delta_s \rceil$. Let $Z_n(r)$ be the probability distribution of the difference between the number of backoff slots in the current contention round and the gap. Such a probability can be expressed as the convolution between $T_n(.)$ and $G(.)$. With abuse of notation, we extend the definition of $T_n(i)$ by setting $T_n(i) = 0$ for $i < 0$. We can then express $Z_n(r)$ as $\sum_{l=0}^{\lceil \Delta_s \rceil - 1} T_n(r + l)/\lceil \Delta_s \rceil$, with $r \in \{-\lceil \Delta_s \rceil + 1, \ldots, CW_n\}$. The backoff evolution process can be characterized as

$$B_n(j) = B_n(j) \cdot \sum_{r=-\lceil \Delta_s \rceil}^{0} Z_n(r-1) + \\ \sum_{r=1}^{CW_n - j} B_n(j+r) \cdot Z_n(r-1) + \\ + \frac{1}{CW_n} \cdot \sum_{r=0}^{CW_n} B_n(r) \cdot \left[1 - \sum_{l=0}^{r-1} Z_n(l) \right]. \tag{4}$$

At the end of each contention round, the backoff counter of the tagged NR-U node n may be equal to j for three different reasons:

- it is equal to the previous contention value, because other nodes transmit before the gap expiration and the backoff process is not resumed;
- it has been decremented to j starting from a greater value $j + r$ because a transmission attempt was performed by other nodes after r slots from the gap expiration;
- it has been randomly set to a value equal to j after the backoff counter of the tagged node was resumed and decremented to zero.

4.1.2. Contention idle time

The medium access process can be characterized as a function of the backoff probability distributions of the contending nodes. In case all nodes belonging to the same technology employ the same constant CW value, they will result in the same backoff distribution ($B_w(.)$ or $B_n(.)$).

In each contention round, the probability $Q(i)$ to observe at least i idle slots is given by the probability that all Wi-Fi nodes have a backoff counter greater than i, and all NR-U nodes have the sum of the gap interval and backoff counter greater than i. With abuse of notation, let $B_n(l) = 0$ for $l < 0$, and let $E_n(r) = \sum_{l=0}^{\lceil \Delta_s \rceil - 1} B_n(r - l)/\lceil \Delta_s \rceil$ be the probability that the sum between the gap interval and the NR-U backoff counter expires within slot r. It follows that

$$Q(i) = \left(\sum_{j=i+1}^{CW_w} B_w(j) \right)^{N_W} \cdot \left(\sum_{j=i+1}^{CW_w} E_n(j) \right)^{N_N}. \tag{5}$$

The probability $Q_h(i)$ that a generic node h observes at least i idle slots in a contention round can be obtained similarly to the previous expression, but removing the tagged node from the set of contending nodes:

$$Q_h(i) = \left(\sum_{j=i+1}^{CW_w} B_w(j) \right)^{N_W - (h==w)} \cdot \left(\sum_{j=i+1}^{CW_w} E_n(j) \right)^{N_N - (h==n)}. \tag{6}$$

where $(h == w)$ and $(h == n)$ are Boolean values, which are equal to 1 when the node uses, respectively, Wi-Fi or NR-U technology. We can now express the probability $T_h(i)$ to have a transmission within the ith backoff slot as:

$$T_h(i) = Q_h(i) - Q_h(i+1). \tag{7}$$

The system of Eqs. (3), (4), (6), and (7) define $B_w(.)$ and $B_n(.)$ as a function of $T_h(.)$, and $T_h(.)$ as a function of $B_w(.)$ and $B_n(.)$. It can then be solved iteratively by means of fixed point iterations. More specifically, the solution is obtained as follows.

Starting from an initial assumption on $B_n(.)$ and $B_w(.)$ distributions, we can readily compute the quantities in (6) and (7). These quantities

are in turn used to update the backoff distributions according to (3) and (4). The backoff distributions are normalized before computing again the idle time distributions $Q_n(.)$ and $Q_w(.)$, as well as the aggregated behavior of other transmission attempts $T_h(.)$. This cycle is repeated until the maximum difference between the probability distributions found in two different iterations is lower than a convergence threshold (set to 0.001 in our implementation).

4.1.3. Performance figures

We focus on the derivation of the probability PS_w (or PS_n) that a Wi-Fi (or NR-U) node successfully transmits in a contention round. We are particularly interested in the analysis of the channel shares obtained by each technology; moreover, the absolute throughput experienced by each node employing a generic technology $h = w, n$ can be easily expressed as a function of its success probability (PS_h), as discussed next. A transmission attempt is successful if a tagged node transmits during the rth slot inside the contention round, while all other nodes are scheduled to transmit after the occurrence of such a slot. Therefore, we can express:

$$PS_w = \sum_{r=0}^{CW_w} B_w(r) Q_w(r+1), \tag{8}$$

$$PS_n = \sum_{r=0}^{CW_n+\lceil \Delta_s \rceil - 1} E_n(r) Q_n(r+1). \tag{9}$$

We can also derive the average number $E[x]$ of idle backoff slots in each contention as:

$$E[x] = \sum_{i=0}^{\min\{CW_h, CW_n+\lceil \Delta_s \rceil - 1\}} i \cdot [Q(i) - Q(i+1)]. \tag{10}$$

The normalized airtime of a given technology is then immediately achievable as:

$$A_H = N_H \cdot \frac{PS_h \cdot L_h}{E[x] \cdot \sigma + E[L]}, \tag{11}$$

where H is the technology (Wi-Fi or NR-U), L_h is the single transmission duration of a node of technology H and $E[L]$ is the average transmission duration over each transmission attempt. For NR-U, L_N is simply the transmission duration, while for Wi-Fi, L_W includes the transmission duration of a DATA frame, one SIFS period, and the transmission duration of an ACK frame. Under the assumption that all collisions last L_N (the transmission duration of a Wi-Fi DATA frame, equal in length to an NR-U transmission), it follows that $E[L]$ can be computed as:

$$E[L] = N_W \cdot PS_w \cdot L_W + N_N \cdot (1 - PS_w) \cdot L_N. \tag{12}$$

4.2. Simulation model

Since the available network simulators lack an implementation of the gap-based approach, we developed our own Monte Carlo simulator of the channel access described in Section 3. We use the simulator to validate the correctness of the analytical model described in Section 4.1 and to generate training data for the regression model described in Section 6. The correctness of the simulator was verified by experiments (cf. Section 5.4).

Following the same assumptions as for the analytical model (no hidden nodes, network saturation, downlink traffic), we design the simulator to iterate over consecutive *contention rounds* (Fig. 2). Each contention round begins after a transmission on the channel completes and consists of:

- a waiting period — needed to resolve the contention, it comprises AIFS, backoff, and gap periods.
- a transmission period (channel holding time) — the node or nodes which won the contention in the waiting period begin their transmissions.

Table 1
Default simulation parameters.

Parameter	Value
Operation band	5 GHz
Wi-Fi CWmin, CWmax	15, 63
NR-U CWmin, CWmax	15, 63
Wi-Fi transmission duration	2 ms
NR-U transmission duration	2 ms
NR-U synchronization slot duration	1000 μs

The duration of the contention rounds is variable, depending on the chosen backoff, data transmission duration, etc. For Wi-Fi, the transmission period excludes the time required for transmitting an acknowledgment (ACK) frame (if a single node won the contention). For NR-U, we assume out-of-band signaling, i.e., that ACKs are transmitted on the licensed channel.

The simulator logic determines which nodes win the contention by calculating the Wi-Fi nodes that have the lowest backoff value and the NR-U nodes that have the lowest backoff and gap value. Next, if the set of nodes that are determined to have won the contention consists of a single node, we consider this a successful transmission. Otherwise, there is a collision. Furthermore, the simulator implements the channel access rules described in Section 3 including channel access parameters, backoff countdown, CW doubling, etc.

Table 1 provides the default simulation parameters (the RS method is straightforward and has no configurable parameters). Once a sufficiently large number (10^5) of contention rounds have elapsed, the simulation ends. The 95% confidence intervals were too small to be displayed.

We measure the following performance metrics:

- **normalized airtime** A — the total channel occupancy time (including ACKs for Wi-Fi and RS for NR-U, if used) related to successful transmissions of either technologies, normalized to the total simulation time,
- **fairness** — measured using Jain's fairness index calculated either over the normalized airtime of each node (simulation model) or over the per-technology average per-node normalized airtime (analytical model),
- **joint airtime-fairness** F — our proposed metric which takes into account both high channel utilization as well as fairness in channel access, calculated as the product of the aggregate normalized airtime of all nodes and the fairness.

5. Observations regarding improving NR-U DL performance

Using the analytical model of Section 4.1 and the simulation model of Section 4.2, we investigate the performance of NR-U and Wi-Fi in a coexistence scenario (configured as described in Table 1) by answering several research questions in the following subsections.

5.1. NR-u synchronization

The first question we posit is: should NR-U nodes (gNBs) remain synchronized when operating on a common shared channel? If all contending gNBs are synchronized in the time domain, e.g., through GPS, then their synchronization slot boundaries start at the same time. Since the gNBs do not use a reservation signal, they will initiate a transmission exactly at the start of their slot boundary. Thus, they are destined to collide. This is corroborated by the results in Fig. 3, where we compare fully synchronized gNBs with desynchronized gNBs (i.e., with randomly offset synchronization slots). The results lead us to formulate the following:

Observation 1. *NR-U gNBs contending in shared channels should be desynchronized.*

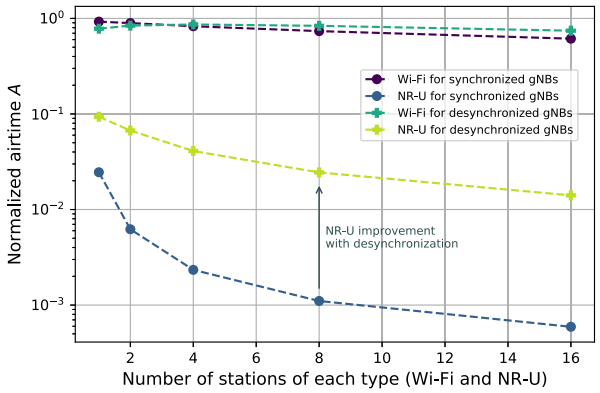

Fig. 3. Simulation results of the impact of gNB synchronization on NR-U performance under coexistence with Wi-Fi.

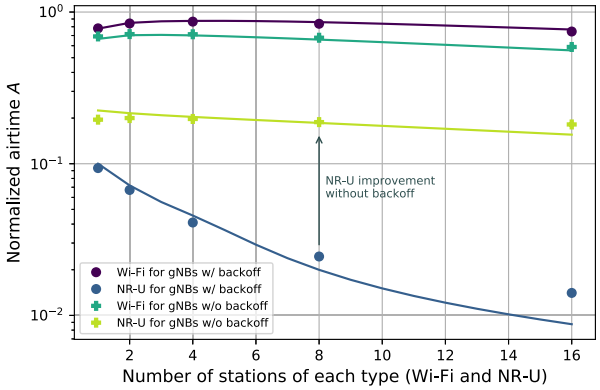

Fig. 4. Impact of disabling backoff at gNBs on NR-U performance under coexistence with Wi-Fi. Solid lines represent analytical model results, points — simulation results.

5.2. Backoff settings of NR-U gNBs

If gNBs are desynchronized (i.e., their slot boundaries start at different times), their transmissions will not be initiated simultaneously. Additionally, they will experience different gap periods in each contention. These two factors render the backoff countdown of LBT unnecessary, as it no longer serves its purpose when the synchronization slot duration is large (1000 μs). We tested this hypothesis by disabling backoff for gNBs (setting CWmin = CWmax = 0). Our results (Fig. 4) confirm that this leads to another improvement in terms of NR-U airtime share.

Observation 2. *Backoff can be disabled for gap-based channel access if the synchronization slot duration is sufficiently large.*

5.3. Equalizing per-technology airtime

Observations 1 and 2 (desynchronizing gNBs and disabling backoff, respectively) have so far provided an improvement in NR-U airtime, but it is still an order of magnitude lower than that of Wi-Fi. This is because both technologies have unequal delay in accessing the channel: (a) Wi-Fi nodes wait for AIFS and the backoff time, (b) NR-U nodes wait for AIFS and a gap time distributed between 0 and the synchronization slot duration, and (c) backoff times are much shorter for Wi-Fi than gap periods for NR-U under the standard parameter set. Furthermore, it is well known that under saturation, appropriately selected constant CWs

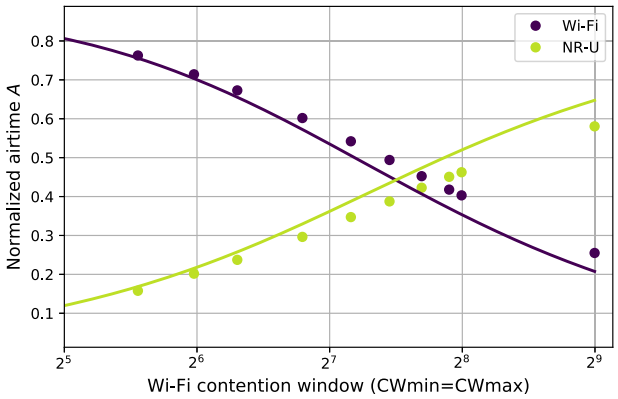

Fig. 5. Example of achieving equal airtime distribution between Wi-Fi and NR-U by equalizing the delay in channel access for $N_W = N_N = 2$ (assuming a fixed $CW_N = 0$). Solid lines represent analytical model results, points — simulation results.

(adjusted to the number of coexisting nodes) can improve performance by avoiding unnecessary collisions [55] while misconfigured CW values lead to unfairness [56]. The analytical and simulation results presented in Fig. 5 provide an example supporting the following:

Observation 3. *It is possible to achieve a fair airtime distribution between Wi-Fi and NR-U by finding the optimal CW settings for both technologies.*

The optimal CW settings can be found using the analytical model of Section 4.1, which can compute the probability to win a contention round and the airtime of each contending node as a function of the contention parameters employed by the coexisting Wi-Fi and NR-U technologies, the synchronization slot of NR-U nodes, and the number of contending nodes belonging to each technology. Let $f(CW_W, CW_N, \Delta_s, N_W, N_N)$ be the model function, whose outputs are PS_W, A_W, PS_N and A_N. Although the function cannot be inverted in a closed form, it is possible to apply a numerical inversion method for adjusting the CW value of a node employing a given technology to achieve a desired airtime. For example, assuming the CW_N value if fixed, it is possible to find the CW_W value which leads to the equalization of airtimes for all contending nodes. Starting from a given $CW_W(n)$ value at step n, considering the relative error on airtimes as a cost function to be set to zero, we can adjust the CW value of Wi-Fi nodes as:

$$CW_W(n+1) = CW_W(n) - \left\lfloor \frac{A_N(n) - A_W(n)}{A_W(n)} \cdot I \right\rfloor, \tag{13}$$

where I is the iteration step (set in our implementation to 64). Exemplary results of this type of CW tuning are shown in Fig. 6 for $N_W = N_N = 2$. Interestingly, the joint airtime-fairness F is maximized for several CW pair values. Therefore, there are no universal CW settings.

Alternatively, simulation or analytical training data can be gathered and a regression model can be used to predict Wi-Fi/NR-U CW settings resulting in a high F, as later described in Section 6.

5.4. Comparison with RS-based channel access

Observations 1–3 have provided us with a configuration profile for Wi-Fi and NR-U, where the latter uses gap-based channel access. How does this profile compare with the case where gNBs use RS-based access? We use the joint airtime-fairness metric, introduced in Section 4.2, to compare the following channel access schemes for NR-U:

- **reservation signal** — gNBs use standard settings and an RS signal prior to transmission,

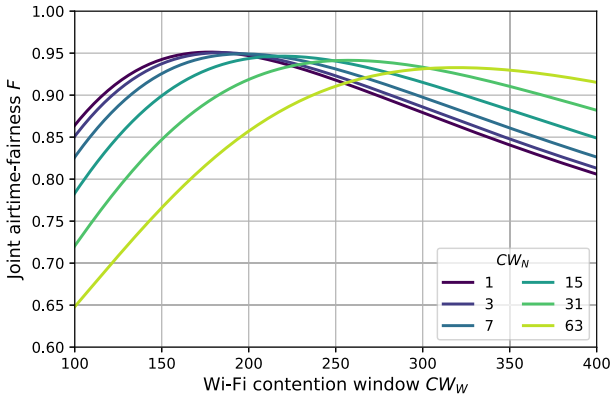

Fig. 6. Maximizing joint airtime-fairness F with different (CW_W, CW_N) pairs for $N_W = N_N = 2$: several pair values lead to similar performance.

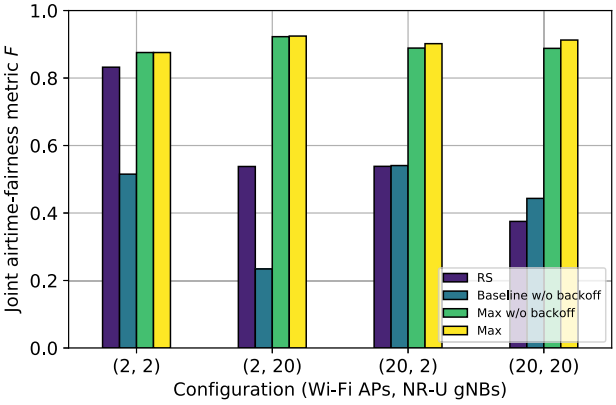

Fig. 7. Simulation results comparing the joint airtime-fairness metric under available channel access approaches: (a) reservation signal (NR-U uses RSs prior to transmission), (b) gap (gNBs do not use RSs, they are desynchronized and backoff is disabled), (c) Wi-Fi CW is optimized (NR-U uses gap settings), (d) both Wi-Fi and NR-U CWs are optimized.

- **gap** — gNBs operate under Observations 1 and 2 (desynchronized, backoff disabled) and wait a gap period prior to transmission,
- **gap with optimal Wi-Fi CW** — gNBs use gap settings but the Wi-Fi CW is optimized for equal channel access,
- **gap with optimal CWs** — gNBs use gap settings and both Wi-Fi and NR-U CWs are optimized.

Fig. 7 presents the simulation results for four different configurations of competing APs and gNBs. The reservation signal approach is the baseline (it also corresponds to the case where Wi-Fi is contending with other Wi-Fi nodes). If gNBs switch from RS to a gap-based approach, the overall network performance is worse (and would be even worse if these nodes were synchronized and used backoff). Fortunately, equalizing the channel access delay by optimizing Wi-Fi's CW settings is enough to considerably improve the performance and surpass even the baseline. Finally, optimizing both Wi-Fi's and NR-U's CW settings leads to an additional improvement. This improvement, however, is minor: NR-U performance is mostly affected by the gap period and, if gNBs are desynchronized, adding a (relatively small) backoff does not provide a meaningful advantage.

In general, optimizing CW leads to values higher than the standard CWmin and this may lead to unwanted increased delay. We measured the channel access delay, defined as the time between the instant a node begins contending for channel access (for a given Wi-Fi data frame or NR-U subframes) and the instant it starts the transmission (or the frame is dropped). Simulations confirmed (results not shown due to the lack of space) that despite the higher CW values, the channel access delay was always lower than the baseline, on account of the reduced collision rate.

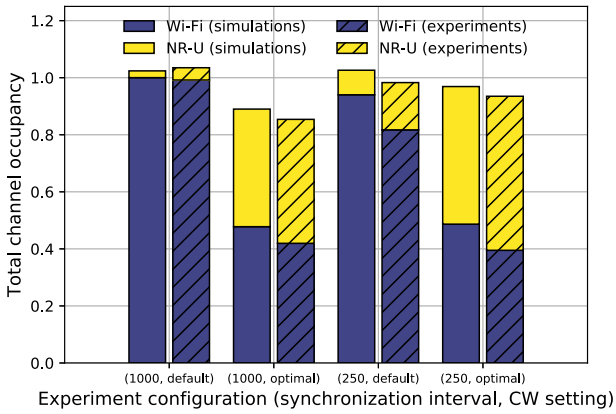

Fig. 8. Comparison of simulation and testbed results.

Observation 4. *The airtime fairness solution arrived at by CW tuning is better in terms of network performance for both Wi-Fi and NR-U than in the case of NR-U using reservation signals.*

We confirmed this observation in our testbed which consists of Wireless open-Access Research Platform (WARP) software defined radios (SDRs). The WARPs are based on field-programmable gate array (FPGA) circuits to exploit both PHY and MAC layer programmability. For Wi-Fi, we used an existing implementation and for NR-U, we implemented its PHY and MAC operation as shown in [10]. At the PHY layer, the Wi-Fi nodes used appropriate transmission rate and frame length settings to achieve a data transmission duration of 2 ms whereas for NR-U we were able to set the transmission duration directly. We used five WARPs, placed in near proximity, to set up the over-the-air validation scenario: two Wi-Fi links composed of a receiver and two transmitters, and two NR-U transmitters. All parameters were configured to replicate the simulation scenario. Fig. 8 presents an airtime metric for both Wi-Fi and NR-U for the two extreme synchronization slots available for NR-U in the 5 GHz band (250 and 1000 μs) and for two CW settings (default and optimal). The airtime metric is the normalized channel occupancy time, defined as all the time nodes using a given channel access method are transmitting (regardless of whether the transmission ended successfully or in a collision) normalized to the total time. Therefore, in this figure, for both simulations and experiments, the metrics include all transmission attempts, i.e., both successful and collided transmissions, which means that it can exceed a value of one. Recall that for NR-U collisions are handled in the licensed bands and it is not always possible to distinguish collisions from successful transmissions while analyzing the unlicensed channel. The presented results both validate the simulation model and show that under optimal CW values the airtime fairness is improved.

5.5. Universal static CW settings

Encouraged by the fact that joint airtime-fairness F can be maximized for different CW pair values (cf. Fig. 6) we looked for static CW settings (CWmin = CWmax) for both technologies that could be considered universal, i.e., exhibiting high performance in a wide range of cases. We used the analytical model of Section 4.1 to generate performance metrics for all combinations of $N_W, N_N \in \{1, 5, 10, 15, 20\}$, $CW_W \in \{32, \ldots, 1024\}$, and $CW_N \in \{0, \ldots, 64\}$. Then, we sorted the

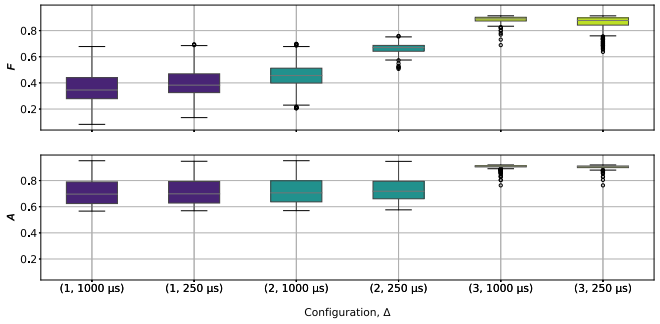

Fig. 9. Box plots of joint airtime-fairness F (top) and normalized aggregate airtime A (bottom) for a varying number of Wi-Fi and NR-U nodes under two different Δ settings (250 µs and 1000 µs) and three CW settings: (1) – standard CW settings for Wi-Fi and NR-U, (2) – standard CW settings for Wi-Fi and backoff disabled for NR-U, (3) – the universal static settings described in Section 5.5.

(CW_W, CW_N) pairs by their F (averaged over all (N_W, N_N) combinations) and selected those with the highest values:

- $CW_W = 319$ and $CW_N = 59$ for $\Delta = 250$ µs,
- $CW_W = 415$ and $CW_N = 19$ for $\Delta = 1000$ µs.

In Fig. 9, we compare the results for three different configurations: (1) standard CW settings for both Wi-Fi and NR-U, (2) standard CW settings for Wi-Fi and backoff turned off for NR-U, and (3) universal static CWS for the following settings: $\Delta \in \{250, 1000\}$ µs, $L = 2100$ µs.[3] The boxes represent the summary of the set of data gathered for a varying number of Wi-Fi and NR-U nodes: $N_W, N_N \in \{1, 2, \ldots, 20\}$. This means that for each box (configuration setting) there were from 2 to 40 nodes transmitting in the network.

For the first configuration, we observe high unfairness in channel access (as discussed in Section 5 and shown in Fig. 3). For the second configuration, the joint airtime-fairness (F) improved, however for large Δ it is still unsatisfactory (as discussed in Section 5 and shown in Fig. 4). For the last configuration, both F and normalized aggregate throughput (A) improved, however, there are several outliers.

Observation 5. *There is no one-size-fits-all CW setting for coexisting Wi-Fi and NR-U networks.*

Since simulations for finding the optimal CW settings for given conditions are time-consuming, in the next section, we demonstrate how a regression model can be used to derive the CW/NR-U parameters, resulting in satisfactory airtime-fairness.

6. Regression model for Wi-Fi/NR-U CW predictions

We have developed a multi-input multi-output regression model for coexisting Wi-Fi and NR-U nodes to predict CW settings resulting in fair channel access under DL transmissions. We used LSTM (Long Short-Term Memory) network-based machine learning, which was successfully applied in the past, e.g., for interference prediction in IoT networks [57].

6.1. Model definition and training

First, we used factorial optimization to find the MAC parameters that impact the quality of Wi-Fi/NR-U coexistence. As a result, the following input parameters were considered: the number of Wi-Fi nodes (N_W), the number of NR-U nodes (N_N),[4] the synchronization period

[3] For $L = 6000$ µs the results and conclusions were similar.

[4] In a practical setting, the values of N_W and N_N can be estimated, e.g., using machine learning with centralized [58] or distributed network monitoring [59], and then exchanged through a centralized controller employing software-defined networking principles [60].

Table 2
Settings of the test configurations.

No.	N_W	N_N	Δ	L	No.	N_W	N_N	Δ	L
1	2	2	250	2.1	13	2	2	250	6
2	2	2	1000	2.1	14	2	2	1000	6
3	2	3	250	2.1	15	2	3	250	6
4	2	3	1000	2.1	16	2	3	1000	6
5	12	2	250	2.1	17	12	2	250	6
6	12	2	1000	2.1	18	12	2	1000	6
7	12	3	250	2.1	19	12	3	250	6
8	12	3	1000	2.1	20	12	3	1000	6
9	24	2	250	2.1	21	24	2	250	6
10	24	2	1000	2.1	22	24	2	1000	6
11	24	3	250	2.1	23	24	3	250	6
12	24	3	1000	2.1	24	24	3	1000	6

length (Δ), and the transmission duration (L). Additionally, CW_W and CW_N were selected as output parameters. Then, we gathered 40,800 samples (from both the analytical model described in Section 4.1 and the simulator described in Section 4.2) for the following settings: $N_W, N_N \in \{1, 5, 10, 15, 20\}$, $CW_W \in \{31, 63, \ldots, 511, 575, \ldots, 1023\}$ (24 settings in total), $CW_N \in \{0, 3, 7, 11, \ldots, 63\}$ (17 settings in total), $\Delta \in \{250, 1000\}$ µs, $L \in \{2.1, 6\}$ ms. Finally, we pruned the training data to the 10 best samples for each training configuration. This way, we obtained 1,000 final samples for LSTM model training. The first 500 samples represent the results for $L = 2.1$ ms, the latter ones represent the results for $L = 6$ ms.

Next, we implemented a sequential model composed of an LSTM input layer with a Rectified Linear Unit (ReLU) activation function, a dense output layer with a linear activation function, and an Adam optimizer with a mean absolute error (MAE) loss function. The model was implemented using Python and Keras. Then, using grid search, we found the following hyper-parameters: epochs=500, batch size=20, units=500, dropout rate=0.5. This allowed to successfully fit the model to both the training data gathered from the simulator and from the analytical model.

6.2. Testing the regression model

We tested the implemented regression model using the 24 configurations given in Table 2. The CW values predicted by the regression model trained with either analytical (*pred-mod*) or simulation (*pred-sim*) data are presented in Table 3. It can be noticed that for the increasing length of Δ—the CW_W size increases. This is a result of the impact of Δ on the probability of NR-U transmission—with larger Δ this probability decreases because NR-U nodes need to wait longer for the beginning of the synchronization slot boundary. Additionally, the size of CW_N is always smaller than the size of CW_W, because the gap mechanism serves as a partial backoff, as discussed in Section 5, to increase the probability of successful NR-U transmissions.

Additionally, in Fig. 10 for each test configuration, we compare three metrics (per-node throughput, normalized airtime A, and joint airtime-fairness F) obtained with (i) the CW settings predicted by the model trained with the analytical data (given in Table 3 as "Pred-mod"), (ii) the CW settings predicted by the model trained with the simulation data (given in Table 3 as "Pred-sim"), (iii) the best CW settings tuned by the analytical model (given in Table 3 as "Tuned"), and (iv) the best CW settings found by our simulation campaign (given in Table 3 as "Simulated") which resulted with the maximum values for each of the test scenarios. All results are very close to each other.

In some cases, the predicted CW settings differ from the simulated/tuned ones. One of the reasons is that the simulation campaign did not cover all possible CW sizes (since this would be too time-consuming) and for some test scenarios it provided satisfactory, although sub-optimal results. Additionally, the model measured fairness using Jain's fairness index calculated over the per-technology average per-node normalized airtime, and not the normalized airtime of each node used by the simulator.

Table 3
Optimal CW values found using different methods: *predicted* by the regression model, *tuned* using the analytical model of Section 4.1, found as having highest airtime-fairness F using the *simulator* of Section 4.2. The first column represents the test configuration number.

No.	Pred-mod		Pred-sim		Tuned		Simulated		No.	Pred-mod		Pred-sim		Tuned		Simulated	
	CW_W	CW_N	CW_W	CW_N	CW_W	CW_N	CW_W	CW_N		CW_W	CW_N	CW_W	CW_N	CW_W	CW_N	CW_W	CW_N
1	108	6	92	18	63	7	63	7	13	118	35	95	17	127	47	127	31
2	186	28	202	7	159	0	191	3	14	248	19	202	9	191	3	159	0
3	121	30	106	19	95	19	63	0	15	131	37	108	18	159	63	127	27
4	198	7	213	7	191	0	191	0	16	262	20	213	9	191	0	191	3
5	228	44	211	39	255	63	223	55	17	215	36	181	24	255	63	255	63
6	308	19	301	15	287	7	255	3	18	438	36	452	35	511	55	479	39
7	239	45	224	40	255	63	255	55	19	224	37	191	25	255	63	287	63
8	329	20	309	14	319	11	255	3	20	458	38	472	36	511	47	511	43
9	308	51	319	50	319	63	351	63	21	281	42	267	31	319	63	383	63
10	506	31	491	26	574	39	575	31	22	580	41	694	53	702	63	703	55
11	317	52	338	50	319	63	383	63	23	290	43	284	32	351	63	383	63
12	531	33	506	26	574	39	639	39	24	600	42	713	53	702	59	767	63

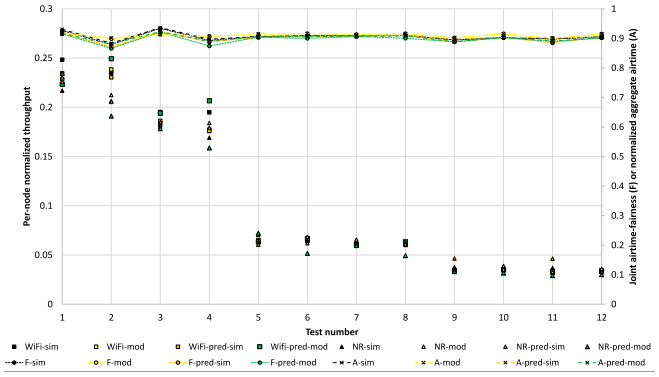

(a) Configurations 1-12

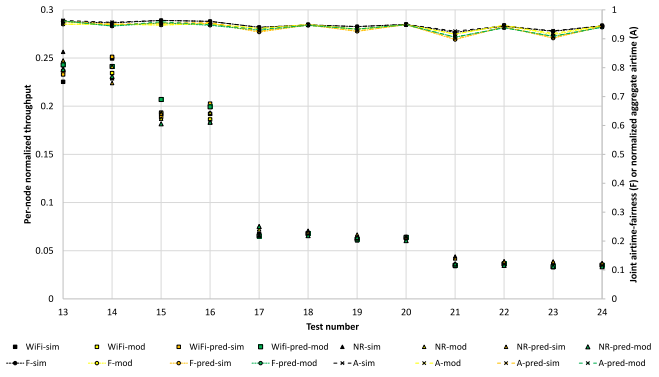

(b) Configurations 13-24

Fig. 10. Comparison of results for CWs predicted by the proposed regression model trained with simulation (*pred-sim*) and analytical data (*pred-mod*), tuned using the analytical model (*mod*), and with the maximum test results (*sim*) for $L = 6$ ms.

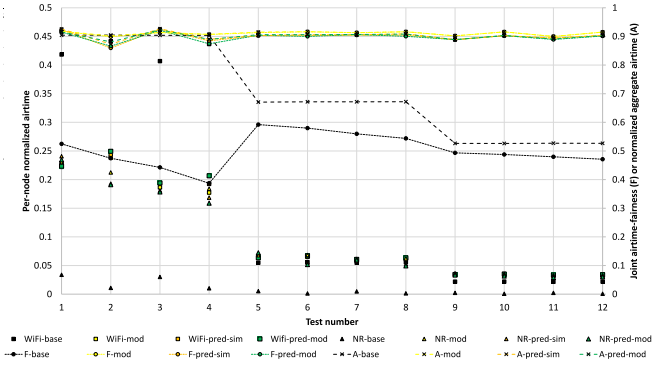

(a) Configurations 1-12

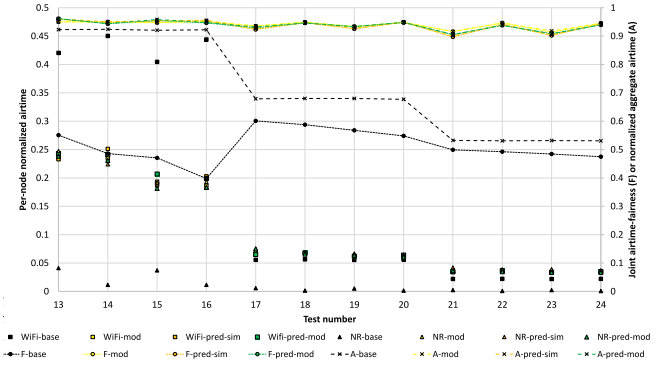

(b) Configurations 13-24

Fig. 11. Comparison of results for CWs predicted by the regression model trained with simulation (*pred-sim*) and analytical (*pred-mod*) data, tuned using the analytical model (*mod*), and with legacy operation (*base*) for $L = 6$ ms.

6.3. Comparison with legacy operation

In Fig. 11, we compare three metrics (per-node throughput, normalized airtime A, and joint airtime-fairness F) obtained using the predicted (pred) and tuned (mod) CW settings with the legacy operation of both Wi-Fi and NR-U (base), i.e., when $C_W^{\min} = C_N^{\min} = 15$ and $C_W^{\max} = C_N^{\max} = 63$. The results confirm the findings from Section 4.2. The proposed approach greatly improves airtime-fairness in channel access for coexisting Wi-Fi and NR-U networks of different size, i.e., the NR-U nodes are no longer outperformed by the Wi-Fi nodes and the A values are higher than for legacy operation. The highest gain in terms of A is observed for a large disproportion in the number of coexisting Wi-Fi and NR-U nodes. For most configurations $F \approx 0.9$ for both the prediction-based and model-based approaches.

Interestingly, for a low number of contending nodes (2, 3 nodes per technology), especially in the case of the larger synchronization period ($\Delta = 1$ ms) and shorter data frames ($L = 2.1$ ms), the operation of Wi-Fi and NR-U technologies does not equalize (cf. configurations 2 and 4 in Fig. 11(a)). This is because for learning we chose samples with the highest F, which is a compromise between fairness in channel access and high channel utilization.

7. Uplink considerations

Hitherto, we have considered only downlink transmissions. In this section, we shift our focus to uplink transmissions. First, we consider Wi-Fi using legacy access (all Wi-Fi stations contend for channel access). We discuss updates to the analytical and simulation models. Then, we conduct a performance analysis to see whether our previous

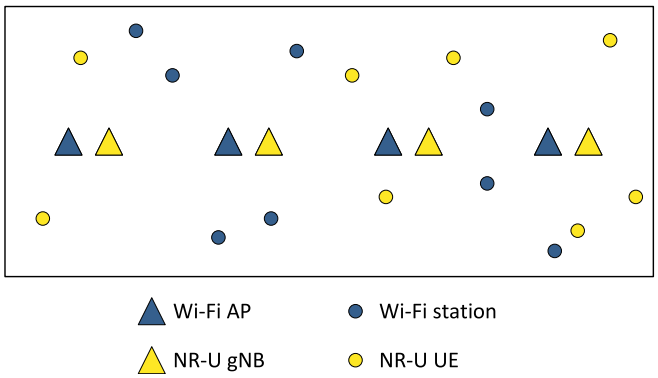

Fig. 12. Layout of 3GPP indoor scenario used for evaluating uplink performance.

Table 4
Uplink simulation parameters.

Parameter	Value
Operation band	5 GHz
Wi-Fi AP CWmin, CWmax	15, 63
Wi-Fi station CWmin, CWmax	15, 1023
NR-U CWmin, CWmax	15, 63
Wi-Fi transmission duration (w/o ACK)	2 ms
NR-U transmission duration	2 ms
NR-U synchronization slot duration	1000 μs
TUA trigger frame (TF) duration	135 μs
TUA MS-BACK duration	487 μs
No. of Wi-Fi APs	4
No. of NR-U gNBs	4

observations still hold. Finding that they do not, we then proceed to analyze the case when Wi-Fi uses TUA (i.e., when only APs contend and schedule all Wi-Fi transmissions).

7.1. Wi-Fi using legacy access

We have updated both the analytical (Section 4.1) and simulation (Section 4.2) models to reflect the following considerations. Instead of downlink transmissions, we only have uplink transmissions in the network. In such a case, Wi-Fi stations can be directly involved in the contention process by independently attempting a channel transmission. Meanwhile, we assume that NR-U stations (user equipment, UEs) can access the channel only within a gNB-initiated frame transmission [42], therefore only gNBs contend for channel access with Wi-Fi stations. If N_{gNB} is the number of gNBs, N_{AP} — the number of Wi-Fi APs, and N_{STA} — the number of stations associated to each Wi-Fi cell, the total number of NR-U contending nodes becomes

$$N_N = N_{gNB} \tag{14}$$

and the total number of Wi-Fi contending nodes becomes

$$N_W = N_{AP} \cdot N_{STA}. \tag{15}$$

The derivation of the backoff distributions and per-node success probabilities can follow the same approach as in the downlink scenario (Section 4.1), with the only difference that each Wi-Fi contending node w now represents a single Wi-Fi station, rather than a Wi-Fi AP. Additionally, we define a new performance metric: per-cell fairness, calculated over the normalized airtime of all nodes within each cell (Wi-Fi or NR-U).

In the following, we consider the 3GPP indoor scenario from 3GPP TR 36.889 under the assumption that there are no hidden nodes and that the radio channel does not introduce errors (Fig. 12, Table 4). There are four Wi-Fi cells (four APs and their associated stations) and four NR-U cells (four gNBs and their connected UEs). The number of uplink transmitting stations and UEs varies. Since NR-U uses

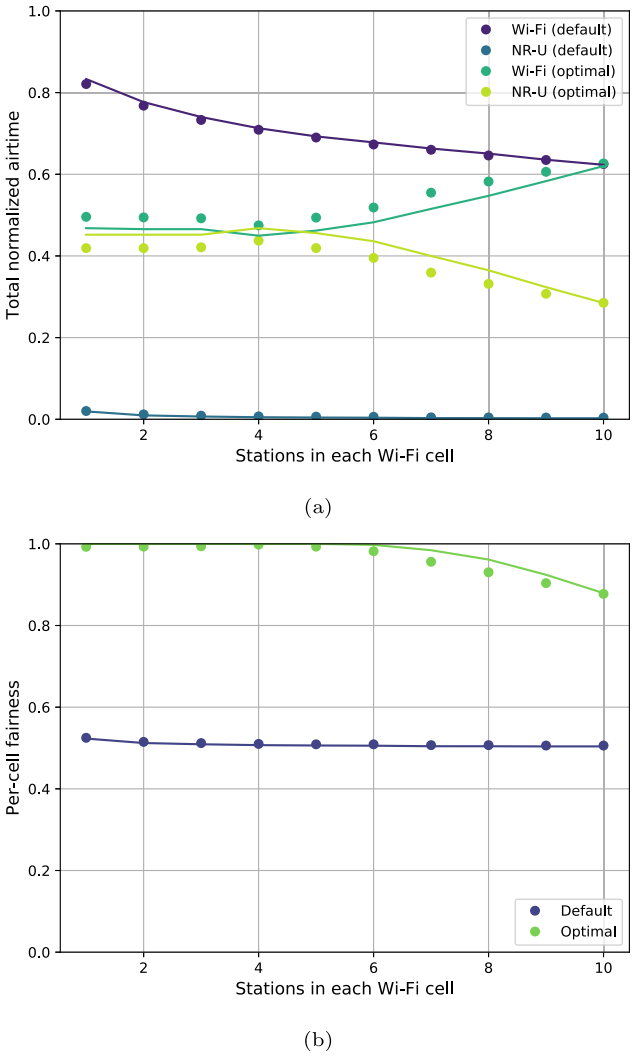

Fig. 13. Uplink performance of Wi-Fi and NR-U coexistence in the 3GPP indoor scenario for default and optimal CW settings: (a) airtime, (b) per-cell fairness. Optimal CW settings were found using the analytical model. Solid lines represent analytical model results, points — simulation results.

gNB-initiated transmissions, the number of UEs does not impact our metrics (aggregate and per-cell airtimes). Thus, the varying number of transmitting Wi-Fi stations is our main input variable.

The results are presented in Fig. 13. For default CW settings, Wi-Fi stations consume almost all available channel airtime. This is reflected in the low per-cell fairness. The Wi-Fi airtime diminishes with the increasing number of stations in each cell on account of the increased collision rate, further reducing the low NR-U airtime share. We then applied our approach of selecting static optimal CW values for both Wi-Fi and NR-U with different CW settings for each network configuration. Using these optimal CW values allowed us to even out the per-technology airtime and achieve fairness close to the optimum. However, our approach is valid only up to a point: once there are more than five stations in each Wi-Fi cell, fairness begins to drop. The explanation for this behavior can be found by looking at the selected optimal CW values: for 6 to 10 stations in each Wi-Fi cell, gNBs are assigned a CW value of zero (the lowest possible), while Wi-Fi stations — the maximum CW value of 1023. Hence, we have reached a limit of CW optimization for the uplink direction.

7.2. Wi-Fi using TUA

The solution to the limitations of CW optimization is to switch to 802.11ax's TUA mode (which uses multi-user orthogonal frequency division multiple access, MU OFDMA) for Wi-Fi uplink transmissions when coexisting with NR-U. This means both technologies would use channel access methods where the coordinator (AP or gNB) triggers uplink transmissions. For Wi-Fi, this increases the signaling overhead by adding a trigger frame before and an extended acknowledgment frame after each data transmission. This is, however, offset by a decreased collision duration when only Wi-Fi APs are involved in the collision.

For TUA, both the analytical (Section 4.1) and simulation (Section 4.2) models need to be slightly extended. If Wi-Fi employs TUA for uplink transmissions, the scenario is equivalent to the downlink one, since only APs contend with gNBs to transmit their trigger frames. Therefore, in both models we now have $N_N = N_{gNB}$ and $N_W = N_{AP}$ and the Wi-Fi transmission duration now has to include the trigger frame duration and have the ACK duration replaced with the multi-station block acknowledgment (MS-BACK) duration:

$$L_W = \text{TF} + \text{SIFS} + \text{DATA} + \text{SIFS} + \text{MS-BACK}. \tag{16}$$

In the simulation model, the collision duration now depends on the type of transmitting stations. In particular, intra-Wi-Fi collisions are shorter (of TF duration). Other collision durations remain the same as before. Meanwhile, in the analytical model, for evaluating the average duration of the contention round, we also have to differentiate between collisions involving only Wi-Fi APs and all the other collisions. Indeed, the time wasted in collision is equal to the longest frame transmitted simultaneously on the channel. Such a time is equal to the trigger frame when NR-U base stations are not involved in the collision. The total percentage of contention rounds leading to a collision (PC) can be easily computed as $PC = 1 - N_W \cdot PS_w - N_N \cdot PS_n$. Meanwhile, the percentage of collisions limited to Wi-Fi stations requires extending the previous analysis by considering the condition that NR-U stations do not transmit. In particular, we need to separately consider the factors leading to the $Q_h(.)$ distribution. Let Q_h^w be the first factor (caused by Wi-Fi stations) and Q_h^n be the second factor (caused by NR-U stations) in (5), which we can specify for Wi-Fi stations as:

$$Q_w^w(i) = \left(\sum_{j=i+1}^{CW_w} B_w(j) \right)^{N_W - 1}, \tag{17}$$

$$Q_w^n(i) = \left(\sum_{j=i+1}^{CW_w} E_n(j) \right)^{N_N}. \tag{18}$$

The percentage of contention rounds TX_w limited to Wi-Fi stations, in which NR-U gNBs do not attempt a transmission, can be expressed as:

$$TX_w = \sum_{i=0}^{CW_w} [Q_w^w(i) - Q_w^w(i+1)] \cdot Q_w^n(i+1), \tag{19}$$

where each term represents the probability that at least one Wi-Fi station transmits in slot i and all NR-U stations have a residual backoff and gap time longer than slot i. In turn, the probability $PS_{w|TX_w}$ that a contention round involving only Wi-Fi stations results in a successful Wi-Fi transmission can be derived as:

$$PS_{w|TX_w} = \sum_{r=0}^{CW_w} B_w(r) Q_w^w(r+1). \tag{20}$$

It follows that the total number of contention rounds PC_w resulting in a collision limited to Wi-Fi stations is:

$$PC_w = [1 - N_W \cdot \sum_{r=0}^{CW_w} B_w(r) Q_w^w(r+1)] \cdot TX_w. \tag{21}$$

Under the assumption that L_N is longer than TF, we can finally derive $E[L]$ as:

$$E[L] = N_W \cdot PS_w \cdot L_W + PC_w \cdot TF +$$

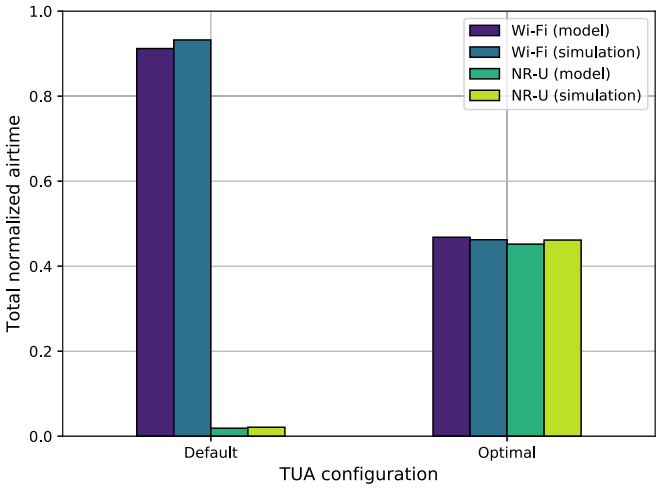

Fig. 14. TUA performance in uplink scenario. Optimal CW settings for the analytical model and simulations were found using the respective tool. The 95% confidence intervals where too small for graphical representation.

$$(1 - N_W \cdot PS_w - PC_w) \cdot L_N. \tag{22}$$

The results in Fig. 14 confirm that, under default CW settings, Wi-Fi transmissions dominate the channel. Moving, however, from default to optimal CW settings allows both technologies to achieve a fair share of the channel airtime. This conclusion is in line with a recent proposal for both Wi-Fi and NR-U to use schedule-based uplink MU OFDMA as a mandatory channel access method in the new 6 GHz band [42]. The proposal considered RS-based gNBs, while we extend this finding to gap-based gNBs (albeit under optimized CW settings).

8. Conclusions

Inspired by the growing interest in assuring coexistence fairness between random (e.g., Wi-Fi) and scheduled (e.g., LTE-LAA, NR-U) wireless networks implementing LBT channel access, in this paper we proposed a re-evaluation of the reservation-less gap mechanism. We showed that by treating gap periods as a partial backoff, it is possible to preserve fairness in coexistence and to avoid the necessity of implementing reservation signals in 5G networks.

Having developed both analytical and simulation models, we validated them in a testbed to show the advantages of our proposed approach. Additionally, we have shown how the analytical model could be used to tune the CW settings for Wi-Fi and NR-U. Furthermore, we developed an LSTM-based regression model to show that it is possible to derive Wi-Fi/NR-U CW values resulting in satisfactory joint fairness-airtime coexistence in practice.

We have also observed that for downlink transmissions it is enough to perform appropriate CW tuning to obtain high per-node and per-cell fairness. In the case of uplink transmissions, this is no longer possible, since it does not allow to compensate both collisions resulting from the increasing number of nodes and the discrepancy between the channel access mechanisms of Wi-Fi and NR-U. As a remedy to this problem, we propose to use triggered uplink access at the Wi-Fi side, combined with the proposed CW tuning. We have shown that this approach provides a fair share of the channel airtime for both technologies.

Finally, we remark that the proposed approach is especially useful for long synchronization periods (i.e., the lengths allowed for NR-U in the 5 GHz band), since for short synchronization periods (symbol-based scheduling) the behavior of Wi-Fi and NR-U converges [10]. However, it remains to be seen whether such symbol-based scheduling can be implemented in practical NR-U deployments. As future work, we plan to consider partially overlapping networks (with hidden nodes) as well

as online learning frameworks [61]. We hope that the presented models and the proposed solution can attract further research and influence future generations of Wi-Fi and NR-U devices.

CRediT authorship contribution statement

Szymon Szott: Conceptualization, Methodology, Software, Investigation, Writing – original draft, Visualization, Supervision. **Katarzyna Kosek-Szott:** Conceptualization, Methodology, Software, Investigation, Writing – original draft, Visualization, Project administration. **Alice Lo Valvo:** Methodology, Software, Validation, Writing – original draft. **Ilenia Tinnirello:** Conceptualization, Methodology, Software, Investigation, Writing – original draft, Visualization, Supervision.

Declaration of competing interest

The authors declare that they have no known competing financial interests or personal relationships that could have appeared to influence the work reported in this paper.

Acknowledgment

This work was carried out as part of project no. DEC-2018/30/M/ST7/00351 financed by the National Science Centre, Poland.

References

[1] V. Sathya, M.I. Rochman, M. Ghosh, Measurement-based coexistence studies of LAA & Wi-Fi deployments in Chicago, IEEE Wirel. Commun. 28 (1) (2021) 136–143, http://dx.doi.org/10.1109/MWC.001.2000205.

[2] V. Sathya, M.I. Rochman, M. Ghosh, Hidden-nodes in coexisting LAA & Wi-Fi: a measurement study of real deployments, in: 2021 IEEE International Conference on Communications Workshops, ICC Workshops, 2021, http://dx.doi.org/10.1109/ICCWorkshops50388.2021.9473873.

[3] J. Wszołek, S. Ludyga, W. Anzel, S. Szott, Revisiting LTE LAA: Channel access, QoS, and coexistence with WiFi, IEEE Commun. Mag. 59 (2) (2021) 91–97, http://dx.doi.org/10.1109/MCOM.001.2000595.

[4] I. Tinnirello, P. Gallo, S. Szott, K. Kosek-Szott, Impact of LTE's periodic interference on heterogeneous Wi-Fi transmissions, IEEE Commun. Lett. 23 (2) (2018) 342–345.

[5] P. Kutsevol, V. Loginov, E. Khorov, A. Lyakhov, New collision detection method for fair LTE-LAA and Wi-Fi coexistence, in: 2019 IEEE 30th Annual International Symposium on Personal, Indoor and Mobile Radio Communications, PIMRC, 2019, pp. 1–6.

[6] 3GPP, LTE; physical layer procedures for shared spectrum channel access (release 16), Technical Specification (TS), (37.213) 3rd Generation Partnership Project (3GPP), 2020, Version 16.4.0.

[7] P. Nikolich, Liaison statement to 3GPP from IEEE 802 LMSC, IEEE 802.19-16/0037r9, IEEE 802, 2016, URL https://mentor.ieee.org/802.19/dcn/16/19-16-0037-09-0000-laa-comments.pdf.

[8] V.A. Loginov, A.I. Lyakhov, E.M. Khorov, Coexistence of Wi-Fi and LTE-LAA networks: Open issues, J. Commun. Technol. Electron. 63 (12) (2018) 1530–1537, http://dx.doi.org/10.1134/S1064226918120148.

[9] M. Cierny, T. Nihtila, T. Huovinen, M. Kuusela, F. Chernogorov, K. Hooli, A. Toskala, Fairness vs. Performance in rel-13 LTE licensed assisted access, IEEE Commun. Mag. 55 (12) (2017) 133–139.

[10] K. Kosek-Szott, A. Lo Valvo, S. Szott, P. Gallo, I. Tinnirello, Downlink channel access performance of NR-U: Impact of numerology and mini-slots on coexistence with Wi-Fi in the 5 GHz band, Comput. Netw. 195 (2021) 108188.

[11] I. Tinnirello, A. Lo Valvo, S. Szott, K. Kosek-Szott, No reservations required: Achieving fairness between Wi-Fi and NR-U with self-deferral only, in: Proceedings of the 24th International ACM Conference on Modeling, Analysis and Simulation of Wireless and Mobile Systems, in: MSWiM '21, Association for Computing Machinery, New York, NY, USA, 2021, pp. 115–124, http://dx.doi.org/10.1145/3479239.3485680, URL.

[12] A.M. Voicu, L. Simić, M. Petrova, Survey of spectrum sharing for inter-technology coexistence, IEEE Commun. Surv. Tutor. 21 (2) (2019) 1112–1144, http://dx.doi.org/10.1109/COMST.2018.2882308.

[13] U. Challita, M.K. Marina, Holistic small cell traffic balancing across licensed and unlicensed bands, in: 19th ACM International Conference on Modeling, Analysis and Simulation of Wireless and Mobile Systems, in: MSWiM '16, 2016, pp. 166–175.

[14] E. Pei, J. Jiang, Performance analysis of licensed-assisted access to unlicensed spectrum in LTE release 13, IEEE Trans. Veh. Technol. 68 (2) (2019) 1446–1458, http://dx.doi.org/10.1109/TVT.2018.2886332.

[15] A.M. Baswade, L. Beltramelli, F.A. Antony, M. Gidlund, B.R. Tamma, L. Guntupalli, Modelling and analysis of Wi-Fi and LAA coexistence with priority classes, in: 2018 14th International Conference on Wireless and Mobile Computing, Networking and Communications, WiMob, 2018.

[16] M. Mehrnoush, V. Sathya, S. Roy, M. Ghosh, Analytical modeling of Wi-Fi and LTE-LAA coexistence: Throughput and impact of energy detection threshold, IEEE/ACM Trans. Netw. 26 (4) (2018) 1990–2003.

[17] M. Hirzallah, M. Krunz, Y. Xiao, Harmonious cross-technology coexistence with heterogeneous traffic in unlicensed bands: Analysis and approximations, IEEE Tr. Cogn. Commun. Netw. 5 (3) (2019) 690–701.

[18] S. Tuladhar, L. Cao, R. Viswanathan, Fair coexistence of LAA and WiFi in multi-carrier LBT based on joint throughput and airtime fairness, in: 2021 IEEE International Symposium on Dynamic Spectrum Access Networks, DySPAN, 2021, pp. 147–152, http://dx.doi.org/10.1109/DySPAN53946.2021.9677088.

[19] M. Haghshenas, M. Magarini, NR-U and Wi-Fi coexistence enhancement exploiting multiple bandwidth parts assignment, in: 2022 IEEE 19th Annual Consumer Communications Networking Conference, CCNC, 2022, pp. 260–263, http://dx.doi.org/10.1109/CCNC49033.2022.9700517.

[20] J. Zheng, J. Xiao, Q. Ren, Y. Zhang, Performance modeling of an LTE LAA and WiFi coexistence system using the LAA category-4 LBT procedure and 802.11e EDCA mechanism, IEEE Trans. Veh. Technol. 69 (6) (2020) 6603–6618.

[21] Q. Ren, J. Zheng, J. Xiao, Y. Zhang, Performance analysis of an LAA and WiFi coexistence system using the LAA category-4 LBT procedure with GAP, IEEE Trans. Veh. Technol. 70 (8) (2021) 8007–8018, http://dx.doi.org/10.1109/TVT.2021.3089607.

[22] Z. Ali, L. Giupponi, J. Mangues-Bafalluy, B. Bojovic, Machine learning based scheme for contention window size adaptation in LTE-LAA, in: 2017 IEEE 28th Annual International Symposium on Personal, Indoor, and Mobile Radio Communications, PIMRC, 2017, pp. 1–7.

[23] J. Tan, L. Zhang, Y.-C. Liang, D. Niyato, Intelligent sharing for LTE and WiFi systems in unlicensed bands: A deep reinforcement learning approach, IEEE Trans. Commun. 68 (5) (2020) 2793–2808.

[24] S. Mosleh, Y. Ma, J.D. Rezac, J.B. Coder, A novel machine learning approach to estimating KPI and PoC for LTE-LAA-based spectrum sharing, in: 2020 IEEE International Conference on Communications Workshops, ICC Workshops, IEEE, 2020, pp. 1–6.

[25] J.M. de C. Neto, S.F. G. Neto, P.M. de Santana, V.A. de Sousa, Multi-cell LTE-U/Wi-Fi coexistence evaluation using a reinforcement learning framework, Sensors 20 (7) (2020) 1855.

[26] R. Ali, B. Kim, S.W. Kim, H. Kim, F. Ishmanov, (ReLBT): A reinforcement learning-enabled listen before talk mechanism for LTE-LAA and Wi-Fi coexistence in IoT, Comput. Commun. 150 (2020) 498–505.

[27] M. Hirzallah, M. Krunz, Sense-bandits: AI-based adaptation of sensing thresholds for heterogeneous-technology coexistence over unlicensed bands, in: 2021 International Conference on Computer Communications and Networks, ICCCN, 2021, pp. 1–9, http://dx.doi.org/10.1109/ICCCN52240.2021.9522223.

[28] E. Pei, L. Zhou, B. Deng, X. Lu, Y. Li, Z. Zhang, A Q-learning based energy threshold optimization algorithm in LAA networks, IEEE Trans. Veh. Technol. 70 (7) (2021) 7037–7049, http://dx.doi.org/10.1109/TVT.2021.3080832.

[29] Y. Ma, S. Mosleh, J. Coder, Analyzing 5G NR-U and WiGig coexistence with multiple-beam directional LBT, in: 2022 IEEE 19th Annual Consumer Communications Networking Conference, CCNC, 2022, pp. 272–275, http://dx.doi.org/10.1109/CCNC49033.2022.9700690.

[30] S. Szott, K. Kosek-Szott, P. Gawlowicz, J.T. Gómez, B. Bellalta, A. Zubow, F. Dressler, WiFi meets ML: a survey on improving IEEE 802.11 performance with machine learning, IEEE Communications Surveys & Tutorials (2022) http://dx.doi.org/10.1109/COMST.2022.3179242.

[31] S. Saadat, W. Ejaz, S. Hassan, I. Bari, T. Hussain, Enhanced network sensitive access control scheme for LTE–LAA/WiFi coexistence: Modeling and performance analysis, Comput. Commun. 172 (2021) 45–53.

[32] D. Candal-Ventureira, F.J. González-Castaño, F. Gil-Castiñeira, P. Fondo-Ferreiro, Coordinated allocation of radio resources to Wi-Fi and cellular technologies in shared unlicensed frequencies, IEEE Access 9 (2021) 134435–134456, http://dx.doi.org/10.1109/ACCESS.2021.3115695.

[33] M. Han, S. Khairy, L.X. Cai, Y. Cheng, R. Zhang, Reinforcement learning for efficient and fair coexistence between LTE-LAA and Wi-Fi, IEEE Trans. Veh. Technol. 69 (8) (2020) 8764–8776.

[34] Y. Gao, LTE-LAA and WiFi in 5G NR unlicensed: Fairness, optimization and win-win solution, in: 2019 IEEE SmartWorld, Ubiquitous Intelligence Computing, Advanced Trusted Computing, Scalable Computing Communications, Cloud Big Data Computing, Internet of People and Smart City Innovation, SmartWorld/SCALCOM/UIC/ATC/CBDCom/IOP/SCI, 2019, pp. 1638–1643, http://dx.doi.org/10.1109/SmartWorld-UIC-ATC-SCALCOM-IOP-SCI.2019.00292.

[35] C.-Y. Huang, H.-Y. Chen, C.-H. Huang, S.-T. Sheu, T.-W. Chiang, T.-L. Cheng, C.-C. Chang, Listen before receive (LBR) assisted network access in LAA and WiFi heterogeneous networks, IEEE Access 9 (2021) 43845–43861.

[36] S. Lagen, L. Giupponi, Listen before receive for coexistence in unlicensed mmwave bands, in: 2018 IEEE Wireless Communications and Networking Conference, WCNC, 2018, pp. 1–6, http://dx.doi.org/10.1109/WCNC.2018.8377293.

[37] H. Lee, H.J. Yang, Downlink MU-MIMO LTE-LAA for coexistence with asymmetric hidden Wi-Fi APs, IEEE Trans. Mob. Comput. 21 (1) (2022) 93–109, http://dx.doi.org/10.1109/TMC.2020.3003314.
[38] R. Saleem, S.A. Alvi, S. Durrani, Performance-fairness trade-off for Wi-Fi and LTE-LAA coexistence, IEEE Access (2021).
[39] V. Loginov, E. Khorov, A. Lyakhov, I. Akyildiz, CR-LBT: Listen-before-talk with collision resolution for 5G NR-U networks, IEEE Trans. Mob. Comput. (2021) 1, http://dx.doi.org/10.1109/TMC.2021.3055028.
[40] V. Loginov, A. Troegubov, A. Lyakhov, E. Khorov, Enhanced collision resolution methods with mini-slot support for 5G NR-u, IEEE Access 9 (2021) 146137–146152, http://dx.doi.org/10.1109/ACCESS.2021.3122953.
[41] H. Kushwaha, V. Kotagi, S.R. Murthy, On the effects of transmit power control on multi carrier LAA-WiFi coexistence, IEEE Trans. Sustain. Comput. (2021) 1, http://dx.doi.org/10.1109/TSUSC.2021.3132951.
[42] G. Naik, J.-M. Park, J. Ashdown, W. Lehr, Next generation Wi-Fi and 5G NR-U in the 6 GHz bands: Opportunities and challenges, IEEE Access 8 (2020) 153027–153056, http://dx.doi.org/10.1109/ACCESS.2020.3016036.
[43] N. Patriciello, S. Lagen, B. Bojovic, L. Giupponi, NR-U and IEEE 802.11 technologies coexistence in unlicensed mmwave spectrum: Models and evaluation, IEEE Access 8 (2020) 71254–71271.
[44] J. Verboom, S. Kim, Stochastic analysis on downlink performance of coexistence between WiGig and NR-U in 60 GHz band, 2020, arXiv preprint arXiv:2003.01570.
[45] A. Daraseliya, M. Korshykov, E. Sopin, D. Moltchanov, S. Andreev, K. Samouylov, Coexistence analysis of 5G NR unlicensed and WiGig in millimeter-wave spectrum, IEEE Trans. Veh. Technol. 70 (11) (2021) 11721–11735, http://dx.doi.org/10.1109/TVT.2021.3113617.
[46] P. Wang, B. Di, L. Song, Cellular communications over unlicensed mmwave bands with hybrid beamforming, IEEE Trans. Wireless Commun. (2022) 1, http://dx.doi.org/10.1109/TWC.2022.3145868.
[47] L. Wang, M. Zeng, J. Guo, Q. Cui, Z. Fei, Joint bandwidth and transmission opportunity allocation for the coexistence between NR-U and WiFi systems in the unlicensed band, IEEE Trans. Veh. Technol. 70 (11) (2021) 11881–11893.
[48] B. Yin, H. Hu, B. Xi, Q. Liu, Y. Zheng, Z. Zhang, Joint radio resources allocation in the coexisting NR-U and Wi-Fi networks, in: 2021 IEEE 32nd Annual International Symposium on Personal, Indoor and Mobile Radio Communications, PIMRC, 2021, pp. 1532–1538, http://dx.doi.org/10.1109/PIMRC50174.2021.9569466.
[49] 5 GHz RLAN; Harmonised Standard covering the essential requirements of article 3.2 of Directive 2014/53/EU, Broadband Radio Access Networks (BRAN),ETSI, 2017.
[50] IEEE standard for information technology–telecommunications and information exchange between systems local and metropolitan area networks–specific requirements - part 11: Wireless LAN medium access control (MAC) and physical layer (PHY) specifications, in: IEEE Std 802.11-2016, 2016, pp. 1–3534.
[51] A. Mukherjee, J.-F. Cheng, S. Falahati, H. Koorapaty, R. Karaki, L. Falconetti, D. Larsson, et al., Licensed-assisted access LTE: coexistence with IEEE 802.11 and the evolution toward 5G, IEEE Commun. Mag. 54 (6) (2016) 50–57.
[52] M. Zając, S. Szott, Resolving 5G NR-U contention for gap-based channel access in shared sub-7 GHz bands, IEEE Access 10 (2022) 4031–4047, http://dx.doi.org/10.1109/ACCESS.2022.3141193.
[53] B. Bellalta, K. Kosek-Szott, AP-initiated multi-user transmissions in IEEE 802.11ax WLANs, Ad Hoc Netw. 85 (2019) 145–159, http://dx.doi.org/10.1016/j.adhoc.2018.10.021, URL https://www.sciencedirect.com/science/article/pii/S1570870518307613.
[54] I. Tinnirello, G. Bianchi, Rethinking the IEEE 802.11e EDCA performance modeling methodology, IEEE/ACM Trans. Netw. 18 (2) (2009) 540–553.
[55] W. Wydmański, S. Szott, Contention window optimization in IEEE 802.11ax networks with deep reinforcement learning, in: 2021 IEEE Wireless Communications and Networking Conference, WCNC, 2021, pp. 1–6, http://dx.doi.org/10.1109/WCNC49053.2021.9417575.
[56] S. Szott, M. Natkaniec, A.R. Pach, An IEEE 802.11 EDCA model with support for analysing networks with misbehaving nodes, EURASIP J. Wireless Commun. Networking 2010 (2010) 71.
[57] A. Nikoukar, Y. Shah, A. Memariani, M. Güneş, B. Dezfouli, Predictive interference management for wireless channels in the Internet of Things, in: 2020 IEEE 31st Annual International Symposium on Personal, Indoor and Mobile Radio Communications, IEEE, 2020, pp. 1–7.
[58] B. Yang, X. Cao, Z. Han, L. Qian, A machine learning enabled MAC framework for heterogeneous internet-of-things networks, IEEE Trans. Wireless Commun. 18 (7) (2019) 3697–3712.
[59] R. Yin, Z. Zou, C. Wu, J. Yuan, X. Chen, G. Yu, Learning-based WiFi traffic load estimation in NR-U systems, IEICE Trans. Fundam. Electron. Commun. Comput. Sci. 104 (2) (2021) 542–549.
[60] R. Chaparadza, T. Ben Meriem, B. Radier, S. Szott, M. Wodczak, A. Prakash, J. Ding, S. Soulhi, A. Mihailovic, SDN enablers in the ETSI AFI GANA reference model for autonomic management & control (emerging standard), and virtualization impact, in: 2013 IEEE Globecom Workshops, 2013, pp. 818–823, http://dx.doi.org/10.1109/GLOCOMW.2013.6825090.
[61] P. Gawłowicz, A. Zubow, Ns-3 meets OpenAI Gym: The playground for machine learning in networking research, in: 22nd ACM International Conference on Modelling, Analysis and Simulation of Wireless and Mobile Systems, MSWiM 2019, ACM, Miami Beach, FL, 2019, http://dx.doi.org/10.1145/3345768.3355908.